Neuroscience 172 (2011) 366–378

AGE-RELATED DECLINE IN SENSORY PROCESSING FOR LOCOMOTION AND INTERCEPTION

M. FRANÇOIS,[a] A. H. P. MORICE,[a]* J. BLOUIN[b] AND G. MONTAGNE[a]

[a]*Institute of Movement Sciences, CNRS and Aix-Marseille University (UMR 6233)*

[b]*Neurobiology of Cognition Laboratory, CNRS and Aix-Marseille University (UMR 6155)*

Abstract—The ability to control locomotion through the environment and to intercept, or avoid objects is fundamental to the survival of all locomotor species. The extent to which this control relies upon optic flow, visual direction cues or non-visual sensory inputs has long been debated. Here we look at the use of sensory information in young and middle-aged participants using a locomotor-driven interceptive task. Both groups of participants were asked to produce forward displacements in more or less impoverished environments by manipulating a joystick and to regulate, if necessary, their displacement velocity so as to intercept approaching targets. We show that the displacements produced by the middle-aged participants were more nonlinear in comparison with young participants. The errors in the middle-aged group can be accounted for by a constant bearing angle (CBA) model that incorporates a decrease in the sensitivity of sensory detection with advancing age. The implications of this study to a better understanding of the mechanisms underlying the detection of the rate of change in bearing angle are discussed.

Key words: bounded-CBA, aging, interception, virtual reality, locomotion, sensory processing.

What perceptual-motor organization is involved in the control of goal-directed locomotion? This question has motivated a large number of studies over the last decade, which have led to important insights into the underlying mechanisms (e.g., Rushton et al., 1998; Warren et al., 2001; Wilkie and Wann, 2002; Bastin et al., 2006a; Fajen and Warren, 2007). Taken together, these studies have shown that participants can take advantage of the perceptual information available in the perceptual flow produced by their displacements, so as to produce online locomotor adjustments. This perceptual-motor dialogue can be formalized through task-specific laws of control linking a movement parameter to a perceptual information (Warren, 1988, 2006). The underlying idea of such laws, which express the circularity of the relations between information and movement, is that some invariant properties in the perceptual flow specify the current state of the relationship linking an agent to his/her environment. This dynamically updated relationship would allow functional locomotor adaptations to take place, which in turn would modify the perceptual flow, and so on and so forth.

Following this logic, specific laws of control have been shown to account for the regulation behavior of participants performing heading tasks (Warren et al., 2001; Wilkie and Wann, 2003), locomotor pointing tasks (Warren et al., 1986) or interceptive tasks (Chardenon et al., 2004). Interceptive tasks have deserved a special interest, not only because many daily activities rely on the ability to intercept and/or to avoid moving objects (in sport, in driving, or while walking in a crowded street), but also because they can provide insights about the central control of actions characterized by severe spatial-temporal constraints. It has been suggested that individuals intercepting moving targets rely on a law of control (Eq. 1) which links the subjects' acceleration to the rate of change in bearing angle (Chapman, 1968; Chardenon et al., 2002; Lenoir et al., 2002, see Fig. 1). The bearing angle corresponds to the angle subtended by the current position of the target and the direction of the subjects' motion. This type of strategy for controlling self-displacements during interceptive tasks is known as the constant bearing angle (CBA) strategy.

Using the CBA strategy, the moving object will be intercepted if the observer cancels any change in the bearing angle by accelerating or decelerating accordingly. An increase in bearing angle informs the participant that he/she will reach the interception point before the target and tells him/her to decelerate accordingly. Conversely, a decrease in bearing angle informs the participant that the object will reach the interception point before him/her and prompts him/her to accelerate accordingly. Finally when the bearing angle is kept constant, no change in velocity is required to intercept the target. The participant will intercept the moving object if he/she succeeds in maintaining his/her current velocity. The CBA strategy can be modeled by relating the participant's acceleration to the rate of change of the bearing angle, with a damping term allowing the system to match the required value smoothly and to avoid oscillations around the stable state (Fajen and Warren, 2003; Wann and Wilkie, 2004; Bastin et al., 2006a) (Eq. 1).

$$\ddot{Y} = k_1 \times \frac{1}{1+200\times e^{(-10\times t)}} \times \dot{\theta} + k_2 \times \dot{Y} \qquad \text{(Eq.1)}$$

In this equation, $\dot{Y}$ and $\ddot{Y}$ are the participant's speed and acceleration, respectively, $\dot{\theta}$ is the rate of change of the

*Corresponding author. Tel: +33-491172202; fax: +33-491172252.
E-mail address: antoine.morice@univmed.fr (A. H. P. Morice).
Abbreviations: AE, absolute error; CBA, constant bearing angle; IP, interception point; SSE, sum of squares error.

0306-4522/11 $ - see front matter
doi:10.1016/j.neuroscience.2010.09.020

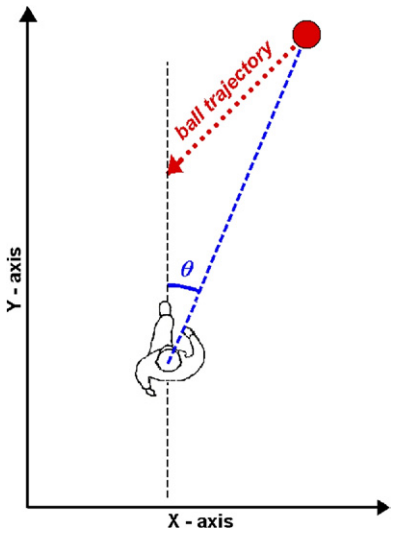

Fig. 1. Bird's eye view of the experimental layout. Participants produced forward displacements on a rectilinear path and aimed to intercept balls that crossed their displacement axis with an angle of 45°. Optical angle of interest is the bearing angle θ. For interpretation of the references to color in this figure legend, the reader is referred to the Web version of this article.

bearing angle, k_1 is a parameter that modulates the strength of the coupling between the acceleration and the rate of change of the bearing angle, and k_2 is a parameter that modulates the strength of the damping term. The function $\frac{1}{1+200\times e^{(-10\times t)}}$ is an activation function.

The use of the CBA strategy has been evidenced in studies which have manipulated task constraints such as ball speed (Lenoir et al., 2002), angle of approach (Chardenon et al., 2005) or ball trajectory curvature (Bastin et al., 2006a). In these studies, the CBA model could explain as much as 80% of the total kinematics variance. Interestingly, the CBA strategy can also explain children's (from 10 to 12 years old) locomotor behavior while intercepting moving balls (Chohan et al., 2008) and locomotion produced by different animal species (fishes, dragonflies) while intercepting prey (Lanchester and Mark, 1975; Olberg et al., 2000).

Since the generalization of the CBA strategy appears well established, recent investigations have focused on the sensory signal that the brain uses for detecting the rate of change in bearing angle. The global optic flow field produced by the moving observer has been identified as a power source of information for detecting this rate of change (*optic flow signals*) (Chardenon et al., 2004). Indeed, because the focus of expansion specifies the direction of the observer's motion, an easy way to detect the bearing angle is to relate the current position of the mobile to the focus of expansion. The detection of the bearing angle remains possible, however, in the absence of optic flow, provided that the observer is able to relate the current position of the object to his/her midline body axis. This egocentric frame of reference is built through the integration of body-related signals, in particular those coming from the vestibular apparatus and from the extra-ocular and neck muscles (Paillard, 1987; Jeannerod, 1991; Blouin et al., 2007). Moreover, the accuracy with which participants refer a moving object with respect to their body can be improved when body-fixed visual references are present in the environment (e.g., a dashboard when driving, a handlebar when cycling; Wilkie and Wann, 2002).

Several studies have been designed to determine how the different sources of information are integrated for detecting the rate of change in bearing angle (Chardenon et al., 2004; Fajen and Warren, 2004). These studies are all based on the same methodology which involves in rendering irrelevant a given source of information (e.g., the focus of expansion no more specifying the actual direction of displacement) and recording the behavioral consequences of this experimental manipulation. Such information manipulation has been achieved, for instance, by laterally displacing the ground plane during self displacement in virtual reality, so as to make irrelevant the position of the focus of expansion (Chardenon et al., 2004), by displacing visual landmarks materializing the midline body axis (Bastin and Montagne, 2005) and by vibrating the neck muscles (Bastin et al., 2006b) in order to bias the egocentric encoding of the target motion direction. Taken together, these studies have shown that the different perceptual signals contribute jointly to the detection of the rate of change in bearing angle. However, the weighting of the signals during this integrative process appears highly context-dependent. The optic flow signal would have the greatest weight when the visual environment is well structured (Bastin and Montagne, 2005; see Warren et al., 2001 for a similar result with heading tasks). In visually impoverished environments, the egocentric frame of reference would gain in importance (Bastin et al., 2006b).

It is worth noting that all the experiments reviewed so far put the emphasis on the perceptual-motor mechanisms allowing young adults to control goal-directed locomotion. In the present experiment, we focused on the much less documented effect of age on these control mechanisms. Aging is generally associated with a decrease in performance in various sensorimotor tasks, including interceptive tasks (Spirduso and MacRae, 1990). This performance decline is known to appear even in moderately advanced age (e.g., 50–60 years, Sarlegna, 2006). Factors contributing to the elders' deficit in intercepting moving objects could include increased perception thresholds in the detection of motion (Warren et al., 1989; Tran et al., 1998; Andersen and Enriquez, 2006) especially for translational motion (Billino et al., 2008). Here we tested whether providing visual information that is known for being informative of the speed and direction of the participant's displacement (e.g., optic flow, body-fixed visual landmark) can help middle-aged adults to compensate, at least partly, for the deteriorating effect of aging during an interception task. We also tested young adults for comparison. The second (related) aim of the experiment was to test to what extent the bearing angle strategy (Eq. 1) could account for the locomotor adjustments produced by the two groups of participants.

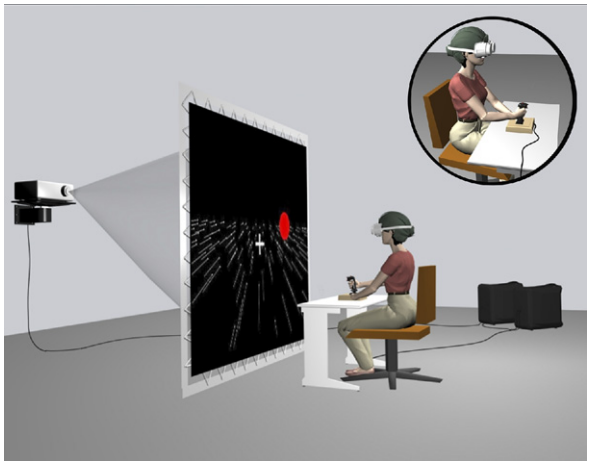

Fig. 2. General overview of the virtual reality set-up. Participants seated in front of a large projection screen and controlled their displacement acceleration via a joystick. Resulting velocity was integrated and coupled to the projected visual scene, so that visual scene displacements were proportional to the participants' current speed. Participants wore goggles that prevented them from seeing the joystick position. For interpretation of the references to color in this figure legend, the reader is referred to the Web version of this article.

EXPERIMENTAL PROCEDURES

Participants

Fourteen females, self-declared right-handed and having normal or corrected-to-normal vision participated to the experiment. They were divided into two experimental groups: Young (n=8, 23.8± 2.1 years old) and Middle-aged (n=6, 57.85±1.95 years old) adults. The subjects gave their informed consent before participating in the experiment. They all had normal or corrected-to-normal vision. A local ethics committee approved the experimental protocol.

Apparatus

The virtual reality set-up (Fig. 2) consisted of two PC Dell workstations (Optiplex GX 240), a joystick (saitick AV8R), a Barco video-Projector (BARCO IQ R500, refreshing rate: 60 Hz) and a 2.3-m high×3-m wide projection screen. The visual scene was projected on the screen, placed 0.70 m in front of the seated participants (providing a 117°×130° field of view). Participants held an analog 2-directions joystick in their right hand with their arm resting on a table. Participants could increase (decrease) their forward acceleration by pushing (pulling) the joystick from the neutral initial position up to an acceleration (deceleration) of 0.75 m/s^2 (−0.75 m/s^2). Resulting speed was bounded from −0.8 m/s to 3.2 m/s, corresponding to the human span of walking speed. When the joystick remained in neutral position, no acceleration or deceleration occurred, allowing to keep the current velocity constant. Participants wore glasses to prevent them from seeing both the joystick and their own hands. The position of the joystick was sampled at 200 Hz and sent to a host computer which computed on-line the position of the participant in the virtual world. From this position data, the visual scene was projected onto the screen by the video projector.

Task and procedure

The experiment was divided into three sessions. The first session allowed the participants to calibrate themselves with the joystick action and with its visual consequences. In this 3-minutes session, participants were immersed in a virtual corridor and were instructed to regulate their velocity so as to keep a constant distance between them and a large virtual textured ball (2 m diameter) rolling on the floor along a straight line at varying velocities (from 0.52 to 3.82 m/s). All participants showed no difficulties in performing this task.

The second session was designed to familiarize the participants with the experimental task. Participants were asked to produce forward displacements in the virtual environment and were instructed to intercept the targets (red untextured spheres, 0.22 m diameter), which moved toward them obliquely (i.e., 45° prior to the participant's displacement) at eye level. They were simply instructed to regulate their velocity in order to intercept the targets with their head when the targets crossed their displacement axis. At the end of each trial, the participants were informed of the distance separating their head from the ball when it crossed their axis of displacement. Positive and negative signs were given when the ball crossed the axis in front or behind the participants, respectively. This session lasted 10 min.

The third session was the experimental session and task requirements remained unchanged compared with the task familiarization session. However, no knowledge of results regarding the participants' performance was provided.

Independent variables

In both the familiarization and experiment tasks, we manipulated the offset of the ball (three levels). The three different offset modalities (−2.5 m, +0.2 m and +2.5 m) corresponded to three different initial ball-to-participant distances along the Y-axis (5.5 m, 8.2 m and 10.5 m). The offset conditions were used to vary the target arrival position along the subject's displacement axis (Fig. 3A), diminishing the possibility of predicting the interception point from the start of the trial, and favoring thus the online control of the displacement velocity. As consequences of the three offsets, keeping the initial displacement velocity (set at 1 m/s) unchanged, would result in the ball passing respectively 0.2 m and 2.5 m in front of the head of the participants for the 8.2 m and 10.5 m initial ball distances, and 2.5 m behind their head in the 5.5 m initial distance.

We also manipulated the visual content of the virtual Environment (four levels) in both the familiarization and experiment tasks. In the so-called *Empty* condition, only the ball was visible (Fig. 3B). In this condition, the bearing angle could only be determined by relating retinal information of the target to extra-retinal signals (e.g., proprioception and oculomotor). In the hereinafter called *Landmark* condition, a grey cross (0.2 m×0.2 m) depicting the midline body axis (which coincided with the axis of displacement) appeared on the screen at about shoulder level. The presence of a body-fixed landmark is believed to enhance the egocentric frame of reference. In the *Ground* condition, the ground plane was textured (extensionless, randomly distributed dots, 0.65 dots/m^2), allowing participants the use of the optic flow to control their displacements. Finally, the cross and the textured ground plane were displayed in the *Full* condition, making available all previously cited visual and non-visual sources of information. The 12 experimental conditions (3 Offsets×4 Environments) were repeated 10 times each, giving rise to a total of 120 trials, randomly presented for each participant. The experimental session lasted approximately 30 min.

Data analysis and dependent variables

The data were analyzed with regard to performance outcome, movement kinematics and perceptual-motor strategies involved.

Performance. Performance was computed in two different ways. The final Y-positions of participants along the Y-axis were cumulated and the percentages of trials displaying undershoots or An overshoots of the interception point (IP) were computed. The

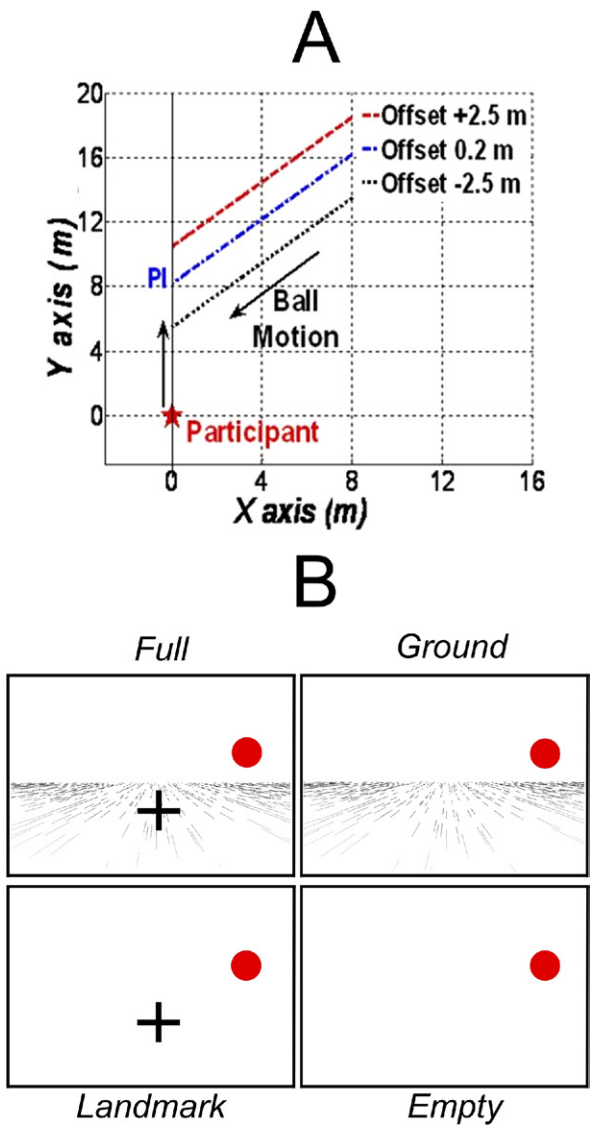

Fig. 3. (A) Bird's eye view of the ball trajectory and interception points (IP) as a function of the three offset conditions (in dotted, plain and dashed lines for the −2.5, +0.2 and +2.5 m offset conditions, respectively). (B) Representation of the different environment conditions (*Empty, Landmark, Ground and Full*). Screenshots are depicted with inversed colors. For interpretation of the references to color in this figure legend, the reader is referred to the Web version of this article.

absolute error (AE) was computed in two different ways. The absolute error was computed as the minimal Euclidian distance between the center of the head and the center of the ball (1) at the moment at which the ball crossed the axis of displacement (i.e., 8 s after the ball appearance) or (2) at any moment during the trial.

Kinematics. The time series of individual velocity ($\dot{Y}$) profiles were averaged over intervals of 500 ms giving rise to 16 time intervals (see Warren et al., 2001; Bastin et al., 2006a, 2008; Morice et al., 2010, for a similar methodology). Individual mean acceleration ($\ddot{Y}$) profiles were also computed and analyzed so as to identify the number of zero-crossings ($ZC_{\ddot{Y}}$). The number of zero crossings reflects the smoothness of a trajectory as it reveals the number of successive acceleration/deceleration cycles during the displacement. For each trial, we picked out the number of zero crossings (from 1 to 5) and we classified the trial accordingly. For each subject, the number of trials found in each category was expressed as a percentage of the total number of $ZC_{\ddot{Y}}$, so as to compare the two groups of participants.

Perceptual-motor strategy. Two types of analyses were performed to test how participants relied on the rate of change of the bearing angle. A rate of change of the bearing angle that remains null during the course of a trial would be in agreement with the use of the CBA strategy. To determine whether the participants used such a strategy to control their displacement during the interceptive task, we first examined the time course of the first derivative of the bearing angle ($\dot{\theta}$) and to what extent their values were kept constant by the young and middle-aged participants. We thus computed the second derivative of the bearing angle ($\ddot{\theta}$) and looked at the time at which it crossed zero ($ZC_{\ddot{\theta}}$)* and also reported the corresponding values of $\dot{\theta}$ at the $ZC_{\ddot{\theta}}$ times.

Subsequent analyses compared the kinematics predicted by the CBA model with the observed kinematics computed by averaging individual displacement velocity profiles recorded for each group. Predicted kinematics were obtained as follow. The best-fitting set of parameters k_1 and k_2 (Eq. 1) were first determined separately for each Offset, Environment and Group. Forty hundred combinations of parameter values were used (k_1 was varied from −0.95 to 0 in increments of 0.05 and k_2 from 0 to 0.95 in increments of 0.05) to solve Eq. 1 with a Runge–Kutta procedure†. The initial mean position and speed of the participant and target were used as input variables. Numerical simulations were done on the complete trial duration (i.e., 8 s). The goodness of the observed data's fits provided by predicted kinematics were investigated through both the percentages of variance accounted for (R^2) and the Sum of Squares Error (SSE) between the predicted and observed curves. Predictions were thus obtained for each group and experimental condition. Secondly, the best set of k_1 and k_2 parameters, common for all offset conditions, but customized to each group and each environment was determined separately by comparing the SSE between best predicted and observed kinematics.

Statistics

For each dependant variable, individual mean values were submitted to analyses of variance (ANOVA).

Discrete variables (absolute error (AE) and zero crossings ($ZC_{\ddot{Y}}$). The effect of both Group and Environment factors on AE and $ZC_{\ddot{Y}}$ individual means were tested with two-ways ANOVAs (2 Groups×4 Environments) with Groups (Young, Middle-aged) as a between-participants factor and Environments (Full, Ground, Landmark and Empty) as a within-participants factor.

Kinematics. Separate three-ways ANOVAs with Environments (Full, Ground, Landmark and Empty), Offsets‡ (−2.5, 0.2 and +2.5) and Time Intervals (16 intervals) as within-participant factors were performed on displacement velocity profiles for each group separately (i.e., Young, Middle-aged).

* Zero-crossings of the second derivative of the bearing angle ($ZC_{\ddot{\theta}}$) reveal changes occurring in the dynamics of the first derivative of the bearing angle.

† We used the automatic step-size Runge-Kutta-Fehlberg integration method provided by the "ode23" Matlab® function.

‡ As mentioned previously, the manipulation of the offset factor was introduced in order to favor the online control of the displacement velocity. As a consequence, no effect of the offset factor on performance was expected and this factor was not included in statistical analyses. Conversely, an effect on kinematics was expected and the factor offset was introduced in the analyses.

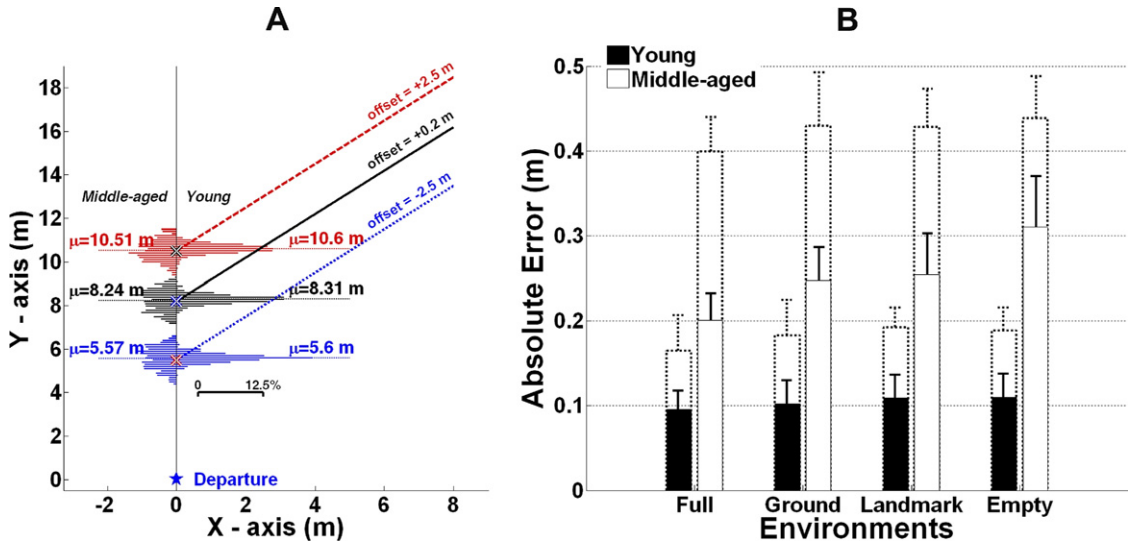

Fig. 4. (A) Frequency distribution of participant's final Y-positions (i.e., participant's positions along the Y-axis at time $t=8$ (s), when the ball crossed the participant's displacement axis) binned each 0.1 m and cumulated across trials performed in the four Environment conditions for the two groups of participants and for the three offset conditions (−2.5, +0.2 and +2.5 m). The distributions of Young and Middle-aged participant's final Y-positions are depicted on the right and left sides of the displacement axis, respectively. The horizontal scale (from 0 to 20%) describes the frequency at which final Y-positions occurred for each bin. The average values of final Y-positions (μ) are reported and depicted with a dotted line. (B) Absolute Error as a function of Environment conditions (Full, Ground, Landmark and Empty) for each Group (Young, Middle-aged). Two computations of Absolute Error are displayed in (B). The dotted bars depict the absolute error computed from the agent-ball distance at time $t=8$ (s). The plain bars represent the absolute error computed from the minimum of the agent-ball distance across the overall time-course of the trial. Vertical bars depict the standard deviation of mean values. For interpretation of the references to color in this figure legend, the reader is referred to the Web version of this article.

Partial effect sizes were computed (η_p^2) and post hoc comparisons were conducted using Newman–Keuls tests. The *P*-value for statistical differences was set at 0.05[§].

Predictions

Because different visual and non-visual sources of information may influence the detection of the rate of change in bearing angle, specific predictions can be made if the participants rely on a CBA strategy depending on the visual content of the environment and the groups of participants. The literature revealed that the different types of perceptual signals are redundant as they allow interceptive tasks to be performed whatever the perceptual content of the environment. Young adults should be able to perform the task with a good accuracy whatever the environment. Middle-aged participants should exhibit a general decrease in their overall performance due to the well-documented increased perception thresholds inducing an impairment in their capacity for detecting motion. Nevertheless, the availability of several sources of information in the rich condition could allow them to compensate, at least partly, this deterioration. Finally it is also reasonable to anticipate that the behavior produced by the middle-aged participants should be jerkier than the behavior produced by young participants.

RESULTS

Performance

The panel A of the Fig. 4 depicts the frequency distributions of participant's final Y-positions (i.e., participant's positions along the Y-axis at time $t=8$ s, when the ball crossed the participant's displacement axis) cumulated across trials for the three offset conditions as compared to the position of the Interception Point (IP equal to 5.5, 8.2 and 10.5 m for the −2.5, +0.2 and +2.5 m Offset conditions). For all Offset conditions, the frequency distributions of young participant's final Y-positions display sharpen peaks, spreading over 0.5 m forward and backward to the IP, whereas the Middle aged distributions of final Y-positions were relatively flat and were spread up to 2 m forward and backward the IP. Distributions of final Y-positions show that, in average, Young participants slightly more overshot the IP (final Y-positions equal to 5.60, 8.31 and 10.6 m) than did Middle-aged participant's (final Y-positions equal to 5.57, 8.24 and 10.51 m). Such overshoot occurred more often for Young participants than for Middle-aged participant's (71.60 vs. 52.47% of trials). More generally, such distributions of trials, in which the IP was sometimes overshot and sometimes undershot (especially for Middle-aged participants) do no indicate a systematic bias toward the IP.

The panel B of Fig. 4 displays the AE computed in two ways for the two groups in the different Environment conditions. We first considered absolute errors as the Euclidian distance between the agent and the ball at the moment at which the ball crossed the participant's displacement axis (dotted bars). This criterion indicated that Young participants were able to intercept the targets with their head at time $t=8$ s as instructed (mean AE equal to 0.18 m) whereas Middle-aged participants were only able to virtually catch the targets with their arms (mean AE equal to 0.42 m). To control that Middle-aged participants succeeded in the task by overcoming the instructions and by

[§] 10% of trials performed by each population were excluded from all analyses (trials with an AE>1.1 m for Young and Middle-aged participants). All remaining trials (successful and unsuccessful) were used in the analyses.

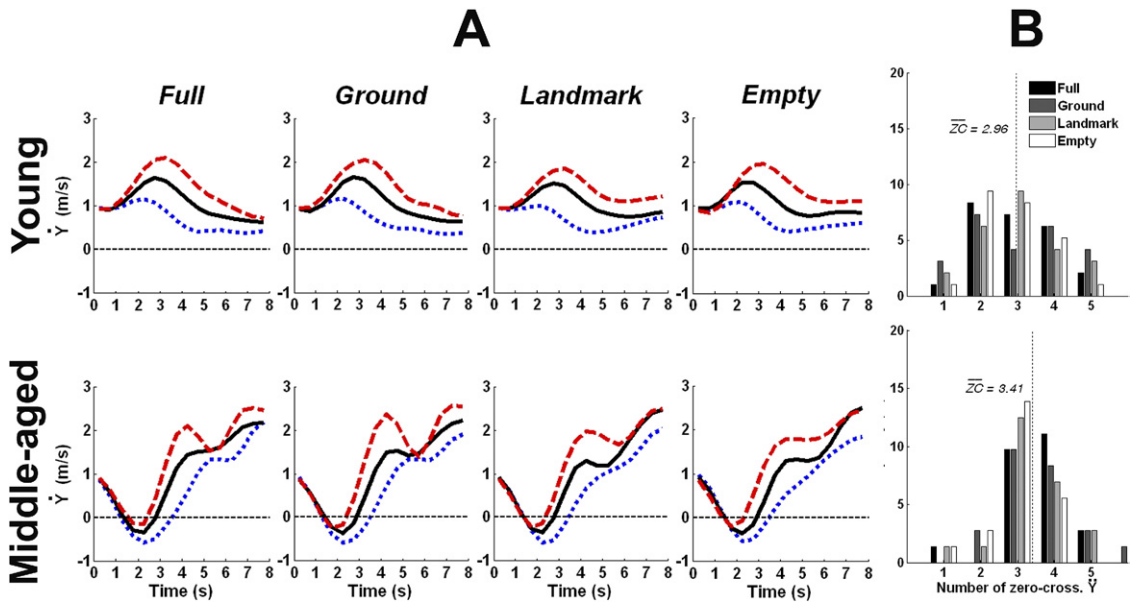

Fig. 5. (A) Displacement velocity profiles exhibited by the two groups of participants (Young, Middle-aged) in the four environment conditions (Full, Ground, Landmark and Empty). (B) Average frequency of zero crossings acceleration ($ZC_{\ddot{Y}}$) occurrence (from 1 to 5 by trial on average) cumulated over participants. The mean values are reported with a dotted line. For interpretation of the references to color in this figure legend, the reader is referred to the Web version of this article.

only attempting to intercept targets at any moment of the trials, we also computed absolute error as the minimum Euclidian distance between the agent and the ball at any moment during the overall trial course (plain bars).

The ANOVA (2 Groups×4 Environments) performed on the AE mean values (computed with the latter definition) revealed a significant main effects of Group ($F_{(1,12)}$= 109.05, $P<.05$, $\eta_p^2=0.90$) and Environment ($F_{(3,36)}=11.33$, $P<.05$, $\eta_p^2=0.49$). The Environment×Group ($F_{(3,36)}=6.76$, $P<.05$, $\eta_p^2=0.36$) interaction was also significant. Post hoc analysis revealed that Young participants were more accurate than Middle-aged participants (0.10±0.01 m *vs.* 0.25±0.04 m) showing thus that, because the latter errors were appreciatively similar to a head diameter, Middle-aged participants succeeded in the task. *A posteriori* comparisons also revealed that, while the performance of Young participants did not significant vary between the different environments ($P>.05$), Middle-aged participants were more accurate in the *Full* environment than in the other environments and were the least accurate in the *Empty* environment (0.20±0.03, 0.25±0.04, 0.25±0.05 and 0.31±0.06 m for the *Full*, *Ground*, *Landmark* and *Empty* conditions, respectively; $P<.05$).

Kinematics

Three-ways repeated measures ANOVAs (4 Environments×3 Offsets×16 Time Intervals) on velocity profiles (Fig. 5A) were performed separately for both groups of participants (*cf.* Table 1).

Young participants. Analyses performed on individual mean velocity profiles revealed significant main effects of Offset ($P<.05$, $\eta_p^2=0.99$) and Time Interval ($P<.05$, $\eta_p^2=0.46$) but no significant main effect of Environment ($P>.05$, $\eta_p^2=0.20$). Moreover, both the Offset×Time Intervals ($P<.05$, $\eta_p^2=0.71$) and Environment×Time Intervals ($P<.05$, $\eta_p^2=0.47$) interactions were also significant. *A posteriori* comparisons revealed that significantly different veloc-

Table 1. Results of the three-ways ANOVAs (4 Environments×3 Offsets×16 Time intervals) performed on displacement velocity separately for each groups of participants (Young, Middle-aged)

	Groups			
	Young		Middle-aged	
	ANOVA	η_p^2	ANOVA	η_p^2
Offset	$F_{(2,14)}=38960.60$, $P>.05$*	0.99	$F_{(2,10)}=1647.37$, $P<.05$*	0.99
Environment	$F_{(3,21)}=1.79$, $P<.05$	0.20	$F_{(3,15)}=8.70$, $P<.05$*	0.63
Time	$F_{(15,105)}=5.98$, $P<.05$*	0.46	$F_{(15,75)}=8.22$, $P<.05$*	0.62
Environment×Offset	$F_{(6,42)}=0.63$, $P>.05$	0.08	$F_{(6,30)}=2.18$, $P>.05$	0.30
Offset×Time	$F_{(30,210)}=16.92$, $P<.05$*	0.71	$F_{(30,150)}=3.12$, $P<.05$*	0.38
Environment×Time	$F_{(45,315)}=6.31$, $P<.05$*	0.47	$F_{(45,225)}=0.97$, $P>.05$	0.11
Offset×Environment×Time	$F_{(90,630)}=0.63$, $P>.05$	0.08	$F_{(90,450)}=0.70$, $P>.05$	0.15

ity profiles were produced in the three Offset conditions during the last 6 s of the trial ($P<.05$) (Fig. 5A). The velocity changes were in accordance with the task requirements, with positive offset condition giving rise to a higher overall displacement velocity in comparison with the negative offset condition, and with intermediate offset condition giving rise to intermediate displacement velocity profiles ($P<.05$). Moreover, Young participants produced similar displacement velocity profiles in all environment conditions ($P>.05$) except during the very last Time interval (i.e., close to ball contact) in which the velocity produced in the *Empty* condition was higher than that produced in the other conditions.

Middle-aged participants. Analyses performed on individual mean velocity profiles revealed significant effects of Offset ($P<.05$, $\eta^2_p=0.99$), Environment ($P>.05$, $\eta^2_p=0.63$) and Time Intervals ($P<.05$, $\eta^2_p=0.62$). Moreover, Offset×Time Intervals ($P<.05$, $\eta^2_p=0.38$) interaction was also significant. *A posteriori* comparisons revealed that significantly different velocity profiles were produced in the three Offset conditions during the last 6 s of the trial ($P<.05$) (Fig. 5A). Once again the velocity changes were in accordance with the task requirements. Moreover it is worth noting that contrary to the other participants, the Middle-aged participants decelerated systematically at the very beginning of the trial, whatever the offset conditions, before producing adaptive velocity changes.

Taken together, these results show that the velocity profiles exhibited by both Young and Middle-aged groups of participants are highly affected by the Offset but only marginally by the Environment. At a more descriptive level, it is also worth noting that the velocity adaptations produced by Young participants are very smooth, contrary to those produced by Middle-aged participants. One can finally notice that the Middle-aged participants sometimes even produced backward displacements in the negative offset condition which was never produced by Young participants.

We further analyzed the displacement kinematics by counting the number of zero crossings ($ZC_{\dot{Y}}$) exhibited in the acceleration profiles. The number of $ZC_{\dot{Y}}$ is indicative of whether the displacement adaptations are gradual (very few $ZC_{\dot{Y}}$) or conversely nonlinear (numerous $ZC_{\dot{Y}}$) (Fig. 5B).

Two-way ANOVA (4 Environments×2 Groups) with repeated measures on the Environment factor performed on the individual mean number of $ZC_{\dot{Y}}$ performed by Young and Middle-aged groups of participants revealed a significant main effect of Group ($F_{(1,12)}=8.62$, $p<.05$, $\eta^2_p=0.42$), but no significant main effect of the Environment factor ($F_{(3,36)}=0.88$, $P>.05$, $\eta^2_p=0.07$). Young participants produced less $ZC_{\dot{y}}$ than the Middle-aged ones (2.97 ± 0.09 *vs.* 3.41 ± 0.21).

Perceptual-motor strategy

In order to investigate to what extent the constant bearing angle strategy can account for the velocity profiles previously described for the two groups of participants, we analyzed the time course of the bearing angle's first derivative ($\dot{\theta}$) for Young (Fig. 6, panel A) and Middle-aged participants (Fig. 6, panel B) in the three offset conditions[‖]. Qualitative inspection of the time course of the rate of change of the bearing angle ($\dot{\theta}$) did not show linear profiles, as predicted by the CBA strategy when intercepting balls approaching along straight paths, but rather wave-like profiles. These $\dot{\theta}$ profiles differed with aging concerning its average values, times at which peaks and valleys occurred and finally amplitudes between peaks and valleys. Concerning the average values of $\dot{\theta}$ profiles, the main panels of Fig. 6 show that whereas Young participants kept in average $\dot{\theta}$ values above zero (around 0.76, 0.96 and 1.00°/s for the −2.5, +0.2 and +2.5 offset conditions, respectively), Middle-aged participants let the values of $\dot{\theta}$ evolving below zeros (around −1.38, −0.99 and −0.67°/s for the −2.5, +0.2 and +2.5 offset conditions, respectively) until the last second of trials. Then, the rate of change of the bearing angle suddenly increased above zero[¶]. Such negative values of the rate of change of the bearing angle during the first 7 s indicate that Middle-aged participants were late compared to the target displacements during the main part of the trials. Note also that the middle values of $\dot{\theta}$ profiles are affected by the offset conditions, especially for Middle-aged participants.

Times at which peaks and valleys occurred in individual $\dot{\theta}$ profiles and amplitudes between these peaks and valleys were then analyzed by computing the zero-crossing exhibited by the second derivative of the bearing angle ($ZC_{\ddot{\theta}}$) in individual profiles. This allowed us to determine when Young and Middle-aged participants conducted $\dot{\theta}$ values toward its average values and to what extent they kept $\dot{\theta}$ values constant.

Times at which peaks and valleys occurred in individual $\dot{\theta}$ profiles were analyzed by plotting bellow each panel of the Fig. 6, the frequency distributions of $ZC_{\ddot{\theta}}$ as a function of corresponding trial time for Young and Middle-aged participants. These distributions of $ZC_{\ddot{\theta}}$ plotted as a function of trial time showed that, when excluding the first and last 0.5 s, Young participants adjusted the $\dot{\theta}$ values at two times (around 3.5 s and 6.5 s) before reaching the interception point. On the other hand, Middle-aged participants performed adjustments of $\dot{\theta}$ values at three times (around 2.5, 4 and 6 s). The frequency distributions $ZC_{\ddot{\theta}}$ as a function of trial time consequently well mirrored the number of zero crossings exhibited by both groups in their acceleration profiles (see previous analyses of $ZC_{\dot{Y}}$).

Amplitudes between peaks and valleys displayed by Young and Middel-aged participants were analyzed by plotting on the right of each panel of the Fig. 6 the frequency distributions of $ZC_{\ddot{\theta}}$ as a function of corresponding

[‖] Given that ball paths were identical and that velocity profiles of Young and Middle-aged did not significantly differ between environment conditions, we averaged the time course of the bearing angle's first derivative across environment conditions at each 0.5 s interval.

[¶] The final asymptote described by the bearing angle's first derivative is an unrealistic artifact that occurs for very near targets due to the use of trigonometrical functions. As a consequence, the features of the bearing angle's first derivative that occurred during the last second of trials were not considered.

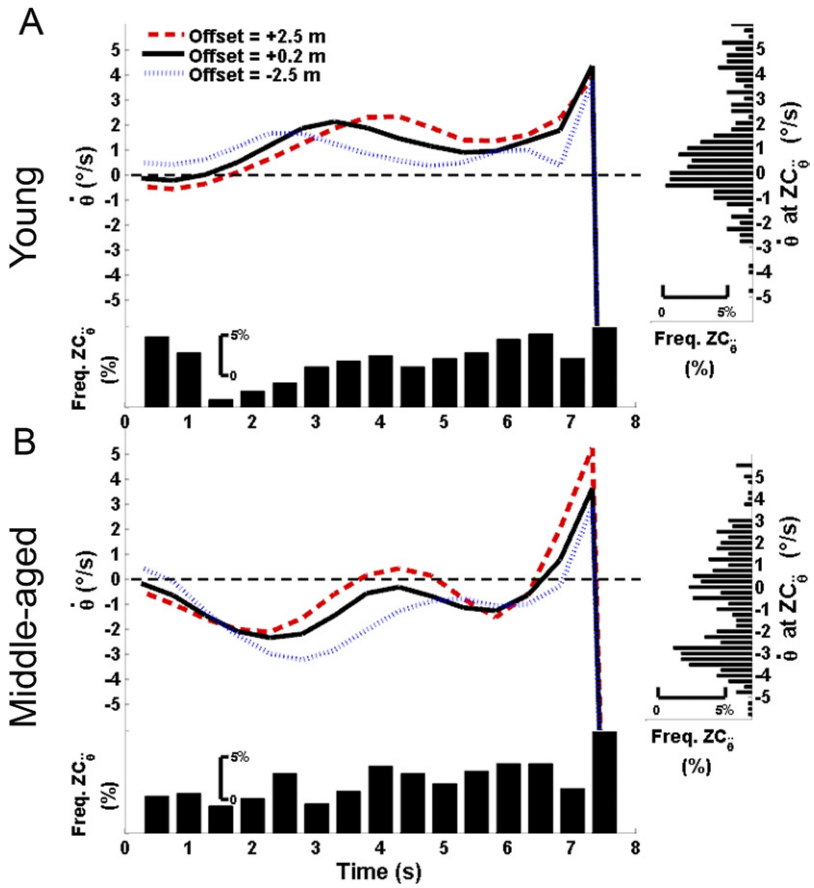

Fig. 6. Time-course over trial time of the bearing angle's first derivative ($\dot{\theta}$, in °/s) averaged across participants and Environment Conditions in the three Offset conditions (in dotted, plain and dashed lines for the −2.5, +0.2 and +2.5 m offset conditions, respectively) for the two Groups of participants (Panel A and B for Young and Middle-aged participants, respectively). Histograms below the X-axis depict the time (binned each 0.5 s) at which the second derivative of the bearing angle ($\ddot{\theta}$) crossed zero ($ZC_{\ddot{\theta}}$). Histograms on the right depict the values of $\dot{\theta}$ (binned each 0.1 °/s) when $ZC_{\ddot{\theta}}$ occurred in individual $\dot{\theta}$ profiles. For interpretation of the references to color in this figure legend, the reader is referred to the Web version of this article.

$\dot{\theta}$ values in individual profiles. Interestingly, the frequency distributions of $ZC_{\ddot{\theta}}$ as a function of $\dot{\theta}$ values display an obvious bimodal distribution for both Young and middle-aged participants, in which higher and lower modes corresponds to the bounds within which $\dot{\theta}$ values are kept during the trial. However, the amplitude between the values of higher and lower modes differs with aging. Indeed, for Young participants, $\dot{\theta}$ values are comprised between higher and lower values equal to +0.75°/s and −0.25°/s. On the contrary, for Middle-aged participants, $\dot{\theta}$ values are comprised between higher and lower values equal to +0.5°/s and −2.75°/s. As a consequence, Young participants allowed $\dot{\theta}$ values to vary within bounds distant of 1°/s whereas Middle-aged participants allowed $\dot{\theta}$ values to vary within bounds distant of 3 °/s. Taken together, these results demonstrate that participants punctually controlled their velocity when the values of $\dot{\theta}$ exceeded some bounds, otherwise the values of $\dot{\theta}$ gradually drifted. This principle allowed participants to keep $\dot{\theta}$ values constant within a window. Because the amplitude spreading the bounds of the windows differed with Age, these results suggest that these windows or bounds can feature some perceptual thresholds, which could be damaged with aging.

Subsequent analyses were based on systematic comparisons between the mean velocity profiles produced by each group of participants and the best fitting numerical simulations provided by the CBA model (Eq. 1). Table 2 summarizes the best-fitting set of parameters (k_1, k_2) and best goodness-of-fit criterions (R^2, SSE) found for each group of participants and for each Environment and Offset conditions. These analyses reveal that the numerical simulations of the CBA model provide a good account of the velocity profiles produced by Young participants in all conditions (R^2 mean values equal to 0.92) (see Table 2, Fig. 7). Conversely, they failed to approximate the regulation behavior exhibited by Middle-aged participants (R^2 mean values equal to 0.56). In particular, it appears that the current version of the CBA model cannot account for their non-gradual velocity profiles.

It is worth noting that the CBA model is based on very simple control architecture and presents a number of shortcomings from a neuro-physiological point of view. For

Table 2. Best-fitting set of parameters (including k_1, k_2 and the perceptual threshold $\dot{\theta}_t$ expressed in °/s) and goodness-of-fit criterions (R^2 and sum of squared errors (SSE) expressed in m^2/s^2) found for each model (CBA and "bounded-CBA") and each group (Young, Middle-aged) in the different environment Conditions (Full, Ground, Landmark and Empty) and in the three Offset conditions (−2.5, +0.2 and +2.5 m). Empty gray cells indicate that $\dot{\theta}_t$ is not taken into account in the CBA model. Goodness-of-fit criterions were evaluated on the 0–7 s trial duration

			Young			Middle-aged		
			$k_1=-0.40$ $k_2=0.30$			$k_1=-0.10$ $k_2=0.10$		
CBA	Environment	Offset	$\dot{\theta}_t$	R^2	SSE	$\dot{\theta}_t$	R^2	SSE
	Full	−2.5		0.94	0.20		fail	9.71
	Full	+0.2		0.89	0.77		0.88	8.18
	Full	+2.5		0.86	1.94		0.82	9.05
	Ground	−2.5		0.94	0.19		fail	9.31
	Ground	+0.2		0.86	0.86		0.83	8.38
	Ground	+2.5		0.86	2.09		0.75	9.36
	Landmark	−2.5		0.84	0.49		fail	8.57
	Landmark	+0.2		0.88	1.04		0.92	8.34
	Landmark	+2.5		0.77	3.36		0.82	8.11
	Empty	−2.5		0.89	0.35		fail	7.88
	Empty	+0.2		0.89	1.01		0.90	8.56
	Empty	+2.5		0.76	3.04		0.85	6.99
	Mean (±std)			0.87 (±0.06)	1.28 (±1.08)		0.56 (±0.42)	8.54 (±0.75)
Bounded-CBA	Environment	Offset	$k_1=-0.60$ $k_2=0.65$			$k_1=-0.45$ $k_2=-0.05$		
	Full	−2.5	1.6	0.95	0.18	2.6	0.90	2.16
	Full	+0.2	1.6	0.96	0.30	2.8	0.96	1.55
	Full	+2.5	1.6	0.96	0.41	3.9	0.90	3.12
	Ground	−2.5	1.6	0.92	0.26	2.6	0.92	1.74
	Ground	+0.2	1.6	0.94	0.34	2.8	0.89	2.31
	Ground	+2.5	1.6	0.96	0.46	3.9	0.94	2.49
	Landmark	−2.5	1.6	0.96	0.14	2.6	0.90	1.73
	Landmark	+0.2	1.6	0.95	0.48	2.8	0.92	1.89
	Landmark	+2.5	1.6	0.84	1.51	3.9	0.95	1.57
	Empty	−2.5	1.6	0.99	0.07	2.6	0.92	1.35
	Empty	+0.2	1.6	0.9	0.66	2.8	0.93	1.85
	Empty	+2.5	1.6	0.85	1.22	3.9	0.91	1.97
	Mean (±std)		1.6	0.93 (±0.05)	0.50 (±0.44)	2.43 (±0.47)	0.92 (±0.02)	1.98 (±0.49)

instance, according to the CBA model, the participant is supposed to cancel any change in bearing angle whatever the magnitude of these changes. This appears as a major limitation for generalizing the model to older populations because the perceptual thresholds are known to increase with aging (Warren et al., 1989; Tran et al., 1998; Andersen and Enriquez, 2006). Adding a perceptual threshold in the perception of the rate of change in the bearing angle could therefore constitute a good way to improve the CBA model and to account for the jerky behavior produced by Middle-aged participants.

This led us to revise the initial formulation of the CBA model (Eq. 1) and to propose a "Bounded-CBA" model (Eq. 2). The "Bounded-CBA" rests on a new, neuro-physiologically grounded, control architecture that comprises two modes. According to this model, the "control" mode gives rise to a behavioral adaptation in velocity each time the rate of change of the bearing angle is greater than a threshold in perceiving $\dot{\theta}$ (thresholds values were deduced from the analyses reported in Fig. 6). Conversely, the "drift" mode is used when angular changes do not exceed the given threshold, and consequently the system maintains the previous velocity until it gets greater than the given threshold, and so on. More precisely, in the "Bounded-CBA" model, the ratio between the current value of the rate of change in bearing angle $\dot{\theta}$ and an assumed perceptual threshold $\dot{\theta}_t$ in perceiving angular change of the bearing angle acts as a switch function that alternatively activates the "control" and "drift" modes. When the absolute value of the ratio $\dot{\theta}/\dot{\theta}_t$ exceeds 1, then the acceleration of the participant ($\ddot{Y}$) is driven by the rate of change in bearing angle and the damping of the system. If the absolute value of the ratio $\dot{\theta}/\dot{\theta}_t$ is less than 1, then the simulated acceleration ($\ddot{Y}$) continues to be gradually driven by the acceleration prescribed at $t-1$.

$$\ddot{Y}=\begin{cases} k_1\times\dfrac{1}{1+200\times e^{(-10\times t)}}\times\dot{\theta}+\ k_2\times\dot{Y}, if\left|\dot{\theta}/\dot{\theta}_t\right|>1 \\ \ddot{Y}_{t-1}, if\left|\dot{\theta}/\dot{\theta}_t\right|<1 \end{cases} \quad \text{(Eq.2)}$$

According to this new bounded-CBA model architecture, for a given set of initial conditions, higher perceptual thresholds should give rise to jerky velocity changes, while low thresholds should give rise to smooth regulations (Fig. 8). A best-fitting procedure identical to the one used for the

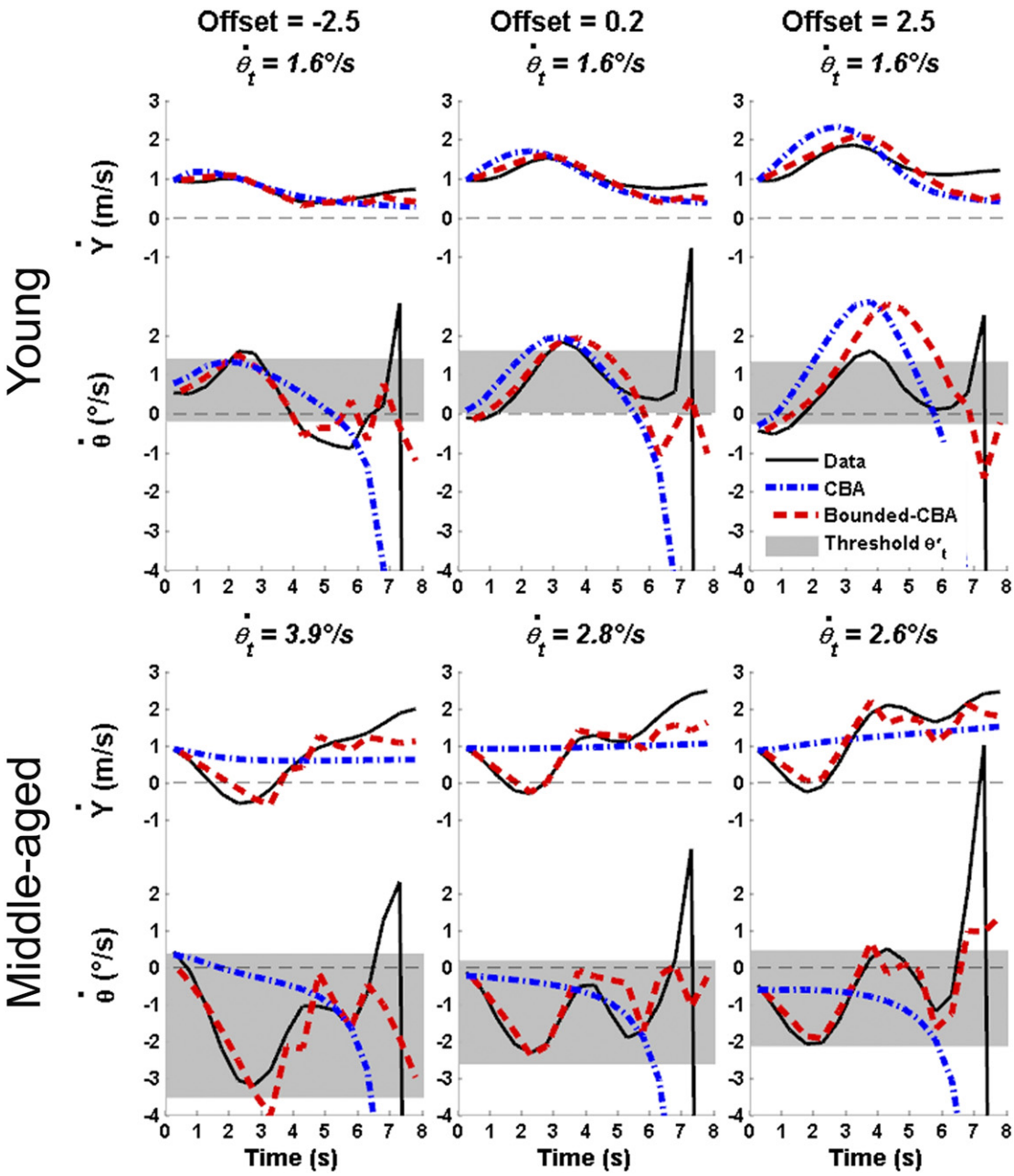

Fig. 7. Average observed velocity ($\ddot{Y}$) and corresponding first derivative of the bearing angle ($\dot{\theta}$) (plain lines) and best fitting numerical simulations provided by the CBA (dotted line) and "Bounded-CBA" models (hatched line) for the two Groups of participants (Young, Middle-aged) in the three offset conditions (−2.5, +0.2 and +2.5 m) for the Empty environment condition. The perceptual thresholds providing the best fit ($\dot{\theta}_t$) are include in title. For interpretation of the references to color in this figure legend, the reader is referred to the Web version of this article.

CBA model was applied to the "Bounded-CBA" model. The parameter k_1 was varied from −0.95 to 0 in increments of 0.05 and k_2 from −0.1 to 0.95 in increments of 0.05 to solve Eq. 2. Moreover we also included a search on the perceptual threshold parameter ($\dot{\theta}_t$) ranging from 0 °/s to 4 °/s with 0.1 °/s increments. The best fitting sets of k_1, k_2 and $\dot{\theta}_t$ values identified in the four Environment and three Offset conditions for the two groups are reported in Table 2. Interestingly, the best perceptual thresholds values accounting for the regulation behavior of both Middle-aged and Young participants greatly differed (3.1 vs. 1.6°/s), but they did not vary very much across the environment conditions. Moreover, numerical simulations of the "Bounded-CBA" model showed that for Middle-aged participants, perceptual thresholds values changed with the Offset conditions (3.8, 2.8 and 2.6°/s for the −2.5, +0.2 and 3 m Offset conditions).

Fig. 7 shows the best-fitting numerical simulations provided by the "Bounded-CBA" model (Eq. 2) for each group of participants and Offset conditions in the *Empty* Environ-

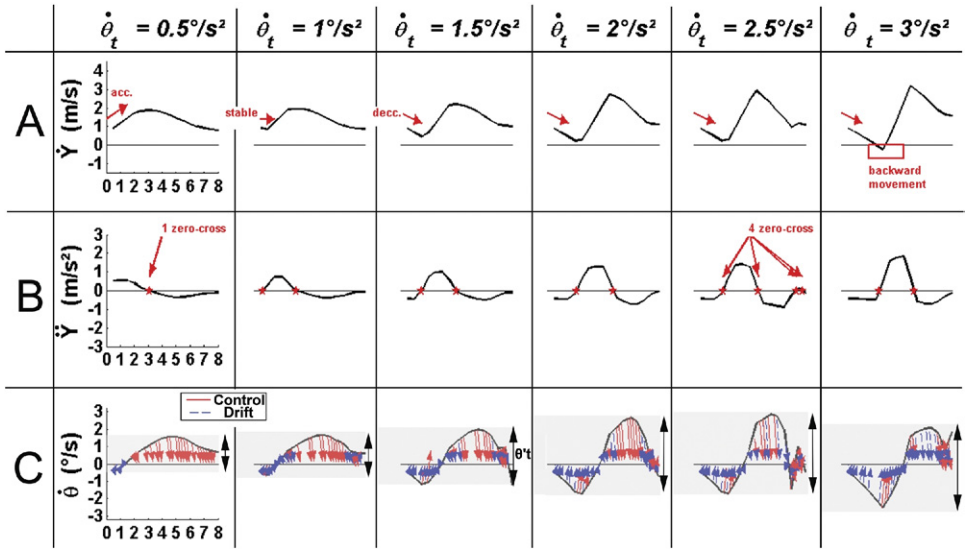

Fig. 8. Numerical simulations of the displacement velocity ($\dot{Y}$, in m/s, Panel A), the corresponding acceleration ($\ddot{Y}$, in m/s, Panel B) and the rate of change of the bearing angle ($\dot{\theta}$, in °/s, Panel C) provided by the "bounded-CBA" model when setting the $\dot{\theta}_t$ boundaries from 0.5 to 3°/s by 0.5°/s steps (from left to right, respectively). Note that initial conditions, k_1 and k_2 parameters remain unchanged in the six simulations. (Panel A) Whereas a $\dot{\theta}_t$ value set at 0.5°/s induces an initial acceleration, increasing the $\dot{\theta}_t$ value to 1°/s induces a stable initial velocity. Setting the $\dot{\theta}_t$ value to 1.5°/s or higher produces an initial deceleration. Finally, critical $\dot{\theta}_t$ values (up to 3°/s) produce not only initial deceleration but also backward displacement. Manipulating only the $\dot{\theta}_t$ value can thus mimic the velocity profiles shown by either Young and Middle-aged participants. (Panel B) The number of zero-crossing of simulated displacement acceleration increases with the $\dot{\theta}_t$ value in a given time. Critical $\dot{\theta}_t$ values (up to 3°/s) induce less zero-crossing due to the limited time of simulation. (Panel C) The arrows depict the influence of the two different modes of control that compete in the "bounded-CBA" model. Red arrows depict a classical control of velocity slaved by the rate of change of the bearing angle. This mode of control occurs punctually when the current value of $\dot{\theta}$ exceeds the assumed perceptual $\dot{\theta}_t$ threshold. Blue arrows represent a second mode of control, called drift, during which the velocity drift until the current value of $\dot{\theta}$ is above the $\dot{\theta}_t$ threshold. The combined influences of both modes of control ("control" and "drift") tend to cancel $\dot{\theta}$. As the $\dot{\theta}_t$ values increases, the balance between the two modes of control tends to become more equally distributed. For interpretation of the references to color in this figure legend, the reader is referred to the Web version of this article.

ment. Contrary to the original CBA model, the "Bounded-CBA" model provides a good account of the velocity profiles not only for Young participants but also for the Middle-aged participants in all conditions (R^2 mean values equal to 0.93 and to 0.92, for Young and Middle-aged participants, see Table 2).

DISCUSSION

We used a virtual reality set-up to assess the effect of age in the control of self-displacement while intercepting moving balls. The two groups of participants (Young, Middle-aged) could be differentiated according to the errors they produced while attempting to intercept the moving ball, but also according to their displacement kinematics. Young participants reached the impact location with greater accuracy than the Middle-aged participants. Moreover, while the Young participants produced smooth displacements whatever the experimental conditions, the Middle-aged participants exhibited jerkier displacements. While being able to explain the regulation behavior of Young participants, the CBA model failed to explain the behavior observed by the Middle-aged participants. Interestingly however, adding adjusted perceptual thresholds in the numerical simulations allowed the model to provide a good account of the behavior produced by the two groups of participants in all environment conditions.

Confirmation of previous studies

The majority of the studies devoted to the understanding of the perceptual-motor mechanisms underlying the control of interceptive actions are derived from studies performed on young and healthy adults (e.g., Lenoir et al., 2002; Chardenon et al., 2004; Fajen and Warren, 2004; Bastin et al., 2008). The results obtained with our Young group are in perfect agreement with the results obtained in these studies. Young participants maintained their high level of performance across the different environment conditions, with smooth velocity adjustments distributed over the entire trial duration. Moreover the Constant Bearing Angle model provided a very good account of these adaptations. The ability of Young participants to maintain their level of performance, even in the more impoverished environment condition, confirms that extra-retinals signals allow the participants to detect the rate of change in bearing angle (Bastin and Montagne, 2005; Bastin et al., 2006b). Including Middle-aged individuals in the present study allows us to determine the effect of a degradation in the processing of visual and non-visual signals on the interception performance.

The influence of aging

The overall decrease in performance exhibited by Middle-aged participants is in agreement with the results obtained

in previous studies (Spirduso and MacRae, 1990); however, these studies have not assessed performance in different visual environments. The present study reveals that the type of environment in which the virtual displacements occurred has an influence on the elders' performance. Remarkably, the condition allowing them to have access to the three types of manipulated perceptual variables (i.e., the *Full* condition) gave rise to the best performance level. Various studies have shown that aging is accompanied by a deterioration of motion detection and perception thresholds (Warren et al., 1989; Morgan and King, 1995; Tran et al., 1998; Andersen and Enriquez, 2006; Zhang et al., 2008), especially for translational motion as in the present study (Billino et al., 2008). It is then reasonable to hypothesize that the detection of the rate of change in bearing angle is easier when redundant information is available. In addition to their failure to intercept the moving ball with the same accuracy as the young adults, the Middle-aged participants clearly exhibited jerkier motion regulation than the Young participants, irrespectively of the environment conditions. We presume that the decline in pure motor functions that is generally observed with aging (e.g., muscular power, Voelcker-Rehage, 2008) cannot account for these decline in elders' performance, as our virtual reality interceptive task put little motor constraints on the participants. The decrease performance of Middle-aged participants in the present study more likely resulted from the slowing of information processing that is generally observed with aging (Welford, 1988; Salthouse, 2000) and the increase motion detection and perception thresholds reported above. In accord with this hypothesis, adding a perceptual threshold in a Bounded version of the CBA model allowed the model to both qualitatively and quantitatively better fit the Middle-aged participants' behavior. It is worth noting that the values of perceptual thresholds determined from average participant's data as well as the values that provided the best fits consistently showed two relevant results. First, a reduced sensitivity to detection of changes in bearing angle was shown for Middle-aged participants. Indeed, Middle-aged adults presented larger range of thresholds than young adults ($\sim$3 °/s and $\sim$ 1 °/s, respectively). Values were found to be similar to those already identified in several psychophysical studies which explored the effect of aging on motion detection, motion perception, angular velocity detection and speed discrimination thresholds of target or vehicle (McKee and Nakayama, 1984; McKee et al., 1986; Bowman and Brown, 1989; Brenner and van den Berg, 1995; Snowden and Kavanagh, 2006). Moreover visual sensitivity to detection of changes in bearing angle was found to be lower for larger initial retinal eccentricity of the ball that had to be intercepted[#], especially for Middle-aged participants. Such effect of the eccentricity of targets was already observed in the literature (Bowman and Brown, 1989; Fhale and Wehrhahn, 1991; Monaco et al., 2007).

[#] In our study, eccentricity was equal to 30.65, 26.28 and 23.38° regarding to the axis of displacement in the −2.5, +0.2 and +2.5 m offset conditions, respectively.

CBA and "Bounded-CBA" models

One of the objectives of the present work was to question the relevance of the constant bearing angle model in accounting for the regulation behavior of Young and Middle-aged participants. One strength of this model is the simplicity of the underlying architecture which links the perceptual information (the rate of change in bearing angle) to an action parameter (the displacement acceleration) with a damping term indexed to the displacement velocity (Eq. 1). While the CBA model has been shown to account for the regulation behavior of Young participants in a very wide range of experimental conditions, the present study challenged the CBA model with Middle-aged participants, presumably presenting neurophysiological deteriorations due to aging. This study shows that a CBA-like model can account for the regulation behavior of Middle-aged participants, provided the architecture of the model incorporates an additional constraint, neurophysiologically grounded. Indeed, adding a perceptual thresholds-like parameter to the CBA model allowed the model to account for the difficulties encountered by the participants to detect the changes in bearing angle (Eq. 2).

CONCLUSION

This study supports the status of the constant bearing angle strategy as a perceptual-motor principle being able to account for the regulation behavior of participants that are characterized with large individual differences and moving in different visual environments. It also illustrates the flexibility of our perceptual systems which provide redundant degrees of freedom allowing the same task to be performed with a good accuracy, whatever the sources of information available. Finally, combining behavioral organizational principles (i.e., CBA strategy) with neurophysiological constraints (i.e., perceptual threshold) is in accord with the increasing trend of the scientific community to propose models that are physiologically grounded.

Acknowledgments—The authors would like to thank Viktor K. JIRSA for its helpful comments concerning mathematical and neurophysiological issues of our modeling work.

REFERENCES

Andersen GJ, Enriquez A (2006) Aging and the detection of observer and moving object collisions. Psychol Aging 21(1):74–85.

Bastin J, Montagne G (2005) The perceptual support of goal-directed displacement is context-dependent. Neurosci Lett 376(2):121–126.

Bastin J, Craig C, Montagne G (2006a) Prospective strategies underlie the control of interceptive action. Hum Mov Sci 25(6):718–732.

Bastin J, Calvin S, Montagne G (2006b) Muscular proprioception contributes to the control of interceptive actions. J Exp Psychol Hum Percept Perform 32(4):964–972.

Bastin J, Jacobs DM, Morice A, Craig C, Montagne G (2008) Testing the role of expansion in the prospective control of locomotion. Exp Brain Res 191(3):301–312.

Billino J, Bremmer F, Gegenfurtner KR (2008) Differential aging of motion processing mechanisms: evidence against general perceptual decline. Vision Res 48(10):1254–1261.

Blouin J, Teasdale N, Mouchnino L (2007) Vestibular signal processing in a subject with somatosensory deafferention: the case of sitting posture. BMC Neurol 7:25.

Bowman KJ, Brown B (1989) Comparison of velocity detection in young and older observers in a simulated night driving situation. Australian government. Department of infrastructure, transport, regional development and local government, 1–8.

Brenner E, van den Berg AV (1995) The special role of distant structures in perceived object velocity. Vision Res 36(23):3805–3814.

Chapman S (1968) Catching a baseball. Am J Physiol 36(10): 868–870.

Chardenon A, Montagne G, Buekers MJ, Laurent M (2002) The visual control of ball interception during human locomotion. Neurosci Lett 334(1):13–16.

Chardenon A, Montagne G, Laurent M, Bootsma RJ (2004) The perceptual control of goal-directed locomotion: a common control architecture for interception and navigation? Exp Brain Res 158(1):100–108.

Chardenon A, Montagne G, Laurent M, Bootsma RJ (2005) A robust solution for dealing with environmental changes in intercepting moving balls. J Mot Behav 37(1):52–64.

Chohan A, Verheul MH, Van Kampen PM, Wind M, Savelsbergh GJ (2008) Children's use of the bearing angle in interceptive actions. J Mot Behav 40(1):18–28.

Fajen BR, Warren WH (2003) The behavioral dynamics of steering, obstacle avoidance, and route selection. J Exp Psychol Hum Percept Perform 29(2):343–362.

Fajen BR, Warren WH (2004) Visual guidance of intercepting a moving target on foot. Perception 33:689–715.

Fajen BR, Warren WH (2007) Behavioral dynamics of intercepting a moving target. Exp Brain Res 180(2):303–319.

Fhale M, Wehrhahn C (1991) Motion perception in the peripheral visual field. Graefe's Arch Clin Exp Ophthalmol 229:430–436.

Jeannerod M (1991) The interaction of visual and proprioceptive cues in controlling reaching movements. In: Motor control: concepts and issues (Humphrey DR, Freund H-J, eds), pp 277–291. New York: Wiley.

Lanchester BS, Mark RF (1975) Pursuit and prediction in the tracking of moving food by a teleost fish (*Acanthaluteres spilomelanurus*). J Exp Biol 63(3):627–645.

Lenoir M, Musch E, Thiery E, Savelsbergh GJP (2002) Rate of change of angular bearing as the relevant property in a horizontal interception task during locomotion. J Mot Behav 34(4):385–401.

McKee SP, Nakayama K (1984) The detection of motion in the peripheral visual field. Visions Res 24(1):25–32.

McKee SP, Silverman GH, Nakayama K (1986) Precise velocity discrimination despite random variations in temporal frequency and contrast. Vision Res 26(4):609–619.

Monaco WA, Kalb JT, Johnson CA (2007) Motion detection in the far peripheral visual field. Report ARL-MR-0684.

Morgan R, King D (1995) The older driver—a review. Postgrad Med J 71:525–528.

Morice AHP, Francois M, Jacobs DM, Montagne G (2010) Environmental constraints modify the way an interceptive action is controlled. Exp Brain Res 202:397–411.

Olberg RM, Worthington AH, Venator KR (2000) Prey pursuit and interception in dragonflies. J Comp Physiol A 186(2):155–162.

Paillard J (1987) Cognitive versus sensorimotor encoding of spatial information. In: Cognitive processing and spatial orientation in animal and man, vol 2 (Ellen P, Blanc-Thinus C, eds), pp 43–77. Dordrecht: Martinus Nijhoff.

Rushton SK, Harris JM, Lloyd M, Wann JP (1998) Guidance of locomotion on foot uses perceived target location rather than optic flow. Curr Biol 8(21):1191–1194.

Salthouse TA (2000) Aging and measures of processing speed. Biol Psychol 54(1–3):35–54.

Sarlegna FR (2006) Impairment of online control of reaching movements with aging: a double-step study. Neurosci Lett 403(3): 309–314.

Snowden RJ, Kavanagh E (2006) Motion perception in the ageing visual system: minimum motion, motion coherence, and speed discrimination thresholds. Perception 35(1):9–24.

Spirduso WW, MacRae PG (1990) Motor performance and aging. In: Handbook of the psychology of aging, vol 3 (Birren JE, Schaie KW, eds), pp 183–200. San Diego: Academic Press.

Tran DB, Silverman SE, Zimmerman K, Feldon SE (1998) Age-related deterioration of motion perception and detection. Graefes Arch Clin Exp Ophthalmol 236(4):269–273.

Voelcker-Rehage C (2008) Motor-skill learning in older adults–a review of studies on age-related differences. Eur Rev Aging Phys Act 5(1):5–16.

Wann JP, Wilkie RM (2004) How do we control high speed steering? In: Optic flow and beyond (Vaina LM, Bdsley SA, Rushton SK, eds), pp 401–420. Dordrecht: Kluwer Academic Publishers.

Warren WH (1988) Action modes and laws of control for the visual guidance of action. In: Complex movement behaviour: '*The*' motor-action controversy (Meijer OG, Roth K, eds), pp 339–380. Amsterdam, NL: North Holland.

Warren WH Jr, Young DS, Lee DN (1986) Visual control of step length during running over irregular terrain. J Exp Psychol Hum Percept Perform 12(3):259–266.

Warren WH Jr, Blackwell AW, Morris MW (1989) Age differences in perceiving the direction of self-motion from optical flow. J Gerontol 44(5):147–153.

Warren WH Jr, Kay BA, Zosh WD, Duchon AP, Sahuc S (2001) Optic flow is used to control human walking. Nat Neurosci 4(2):213–
216.

Warren WH Jr (2006) The dynamics of perception and action. Psychol Rev 113(2):358–389.

Welford AT (1988) Reaction time, speed of performance, and age. Ann N Y Acad Sci 515:1–17.

Wilkie RM, Wann JP (2002) Driving as night falls: the contribution of retinal flow and visual direction to the control of steering. Curr Biol 12(23):2014–2017.

Wilkie RM, Wann JP (2003) Controlling steering and judging heading: retinal flow, visual direction and extra-retinal information. J Exp Psychol Hum Percept Perform 29(2):363–378.

Zhang C, Hua T, Li G, Tang C, Sun Q, Zhou P (2008) Visual function declines during normal aging. Curr Sci 95(11):1544–1550.

(Accepted 14 September 2010)
(Available online 15 October 2010)